Kinetic Rates of Thermal Transformations and Diffusion in Polymer Systems Measured during Sub-millisecond Laser-Induced Heating

Byungki Jung,[†] Jing Sha,[†] Florencia Paredes,[†] Manish Chandhok,[‡] Todd R. Younkin,[‡] Ulrich Wiesner,[†] Christopher K. Ober,[†] and Michael O. Thompson[†,*]

[†]Department of Materials Science and Engineering, Cornell University, Ithaca, New York 14853, United States, and [‡]Intel Corporation, Hillsboro, Oregon 97124, United States

Controlling and differentiating between chemical kinetic processes through temperature and time is critical to synthesis and processing of nearly all materials.[1,2] As kinetic rates increase exponentially with temperature, it is critical to simultaneously reduce the time when increasing temperature to maintain control and stability.[3] For example, in semiconductor junction processing, achieving defect annealing without diffusion has forced processes to shift from furnace anneals at <1000 °C to temperatures approaching ~1250 °C, but for only millisecond time frames.[4] In contrast to such inorganic systems, polymers and small molecules are considerably more fragile and the temperature range available for processing has generally been assumed to be limited,[5] yet high temperatures may offer unique opportunities for processing. Using a transient laser heating source, we are able to characterize and process thermally sensitive organic molecules to temperatures at least 400 °C higher than conventionally accepted limits. In addition, we have characterized chemical kinetic rates over 10 orders of magnitude for a near-solid state system, revealing previously unobserved and unexpected behavior. Identifying and quantifying such fundamental reaction mechanisms, critical to the understanding and processing of small molecule and polymer systems, is now possible over a vastly expanded temperature range.

Millisecond transient thermal annealing, developed to address issues of dopant activation and diffusion,[4] is achieved using a continuous wave (CW) laser focused to a line and scanned over the

ABSTRACT
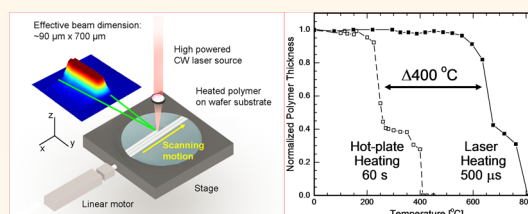
Probing chemical reaction kinetics in the near-solid state (small molecules and polymers) is extremely challenging because of the restricted mobility of reactant species, the absence of suitable analytical probes, and most critically the limited temperature stability of the materials. By limiting temperature exposure to extremely short time frames (sub-millisecond), temperatures in excess of 800 °C can be accessed extending kinetic rate measurements many orders of magnitude. Here we demonstrate measurements on a model system, exploiting the advantages of thin-films, laser heating, and chemically amplified resists as an exquisite probe of chemical kinetic rates. Chemical reaction and acid diffusion rates were measured over 10 orders of magnitude, exposing unexpected and large changes in dynamics linked to critical mechanism shifts across temperature regimes. This new approach to the study of kinetics in near-solid state materials promises to substantially improve our understanding of processes active in a broad range of temperature-sensitive, low-mobility materials.

KEYWORDS: laser spike annealing · chemically amplified resists · side-chain cleavage kinetics · acid diffusion · submillisecond kinetics

surface. The surface temperature rises on time frames of microseconds to milliseconds followed by cooling at similar rates by thermal conduction into the substrate. For these studies, films were irradiated using a CO_2 laser ($\lambda = 10.6\ \mu m$) focused to a 90 μm by 700 μm line beam scanned at velocities of 13−2000 mm/s, as schematically shown in Figure 1. These conditions correspond to dwell times (τ_{dwell}) of 7500−50 μs, defined as the beam full width half-maximum divided by the scan

velocity. In contrast to a hot-plate, the temperature is never entirely isothermal but remains within 5% of the peak temperature for approximately τ_{dwell} and cools to the ambient within $\sim 10\tau_{dwell}$ (see Supporting Information). Although polymers are generally poor thermal conductors ($D_T \approx 10^{-4}$ to 10^{-3} cm^2/s), the characteristic thermal diffusion distance for a 1 ms dwell is >3 μm, resulting in nearly complete equilibration across 100 nm thick films.

To characterize and probe the thermal stability and kinetics of a model near-solid state system, chemically amplified photoresist systems were studied. In these systems, the critical chemical transformation is a cascade of thermally activated side-chain cleavage reactions catalyzed by the diffusion of photochemically generated acids (produced by UV irradiation of small molecule photoacid generators).[2,6] Cleavage of these side-chains modifies the solubility of the polymer in a basic solution resulting in dissolution of exposed areas. This property enables the resist systems to be used as a sensitive monitor of chemical reaction rates. In this article, we report the kinetics of this side-chain cleavage reaction and the diffusivity of the photogenerated acids
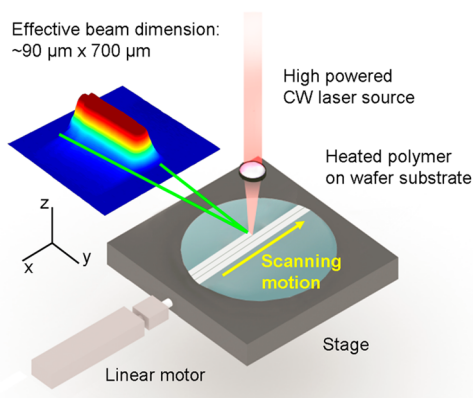

Figure 1. Millisecond heating of a resist polymer using a CO$_2$ laser system. Schematic drawing shows a continuous wave CO$_2$ line beam scanning the substrate in the x direction. The beam is scanned with 100 μm steps to cover large areas. Thermal profile of the beam with a beam dimension of 90 μm by 700 μm is shown.

as a function of both temperature and heating time over the millisecond to second time frames.

The model resist system consists of a copolymer backbone of 2-methyl-2-adamantyl methacrylate-co-γ-butyrolactone-2-yl methacrylate (MAdMA-co-GBLMA, Figure 2a), with a relatively high glass transition temperature ($T_g \approx 160\ °C$).[7] A triarylsulfonium hexafluoroantimonate salt (THS, Figure 2b) was used as the photoacid generator,[8] which reduced the T_g of the copolymer to $\sim 110\ °C$ at 5 wt % loading (see Supporting Information). Poly(MAdMA-co-GBLMA) containing 5 wt % THS was vigorously stirred overnight in propylene glycol monomethyl ether acetate (PGMEA). The prepared solution was spun onto a silicon wafer substrate with 100 nm as the target thickness. All samples were soft baked on a vacuum hot-plate at 130 °C for 90 s to remove the PGMEA solvent. The initial concentration of acids in the film was established by exposing resist-coated wafers to UV irradiation (235−260 nm) at doses of 0.1−12 mJ/cm^2 to activate the THS. Samples were subsequently heated under either isothermal conditions on a vacuum hot-plate or using the submillisecond laser heating system. In the presence of a free acid and sufficient temperature/time, a side-group of MAdMA is cleaved and converted to methacrylic acid, which subsequently regenerates the acid as it stabilizes to methylene adamantane[9] (Scheme 1). Following either hot-plate or laser heating, samples were developed in 0.26 N tetramethylammonium hydroxide (TMAH) for 60 s at room temperature. Three critical properties for this polymer system were measured: the thermal stability of the polymer at extreme temperatures, the side-group cleavage kinetics via dissolution measurements, and diffusion of the photogenerated acids using a bilayer technique.[10,11]

RESULTS AND DISCUSSIONS

To establish the temperature range for polymer characterization and processing in the millisecond time frame, poly(MAdMA-co-GBLMA) without additive ($T_g \approx 160\ °C$) was spin coated on a wafer substrate. Figure 3 shows the thickness remaining as a function of
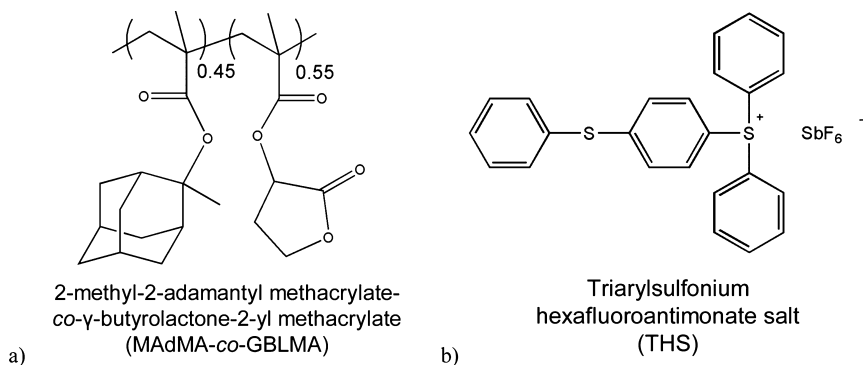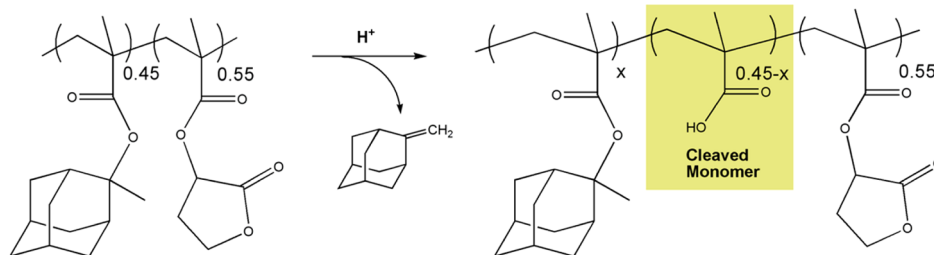

Figure 2. Chemical structures of (a) resist poly(MAdMA-co-GBLMA) (2-methyl-2-adamantyl methacrylate-co-γ-butyrolactone-2-yl methacrylate) and (b) photoacid generator THS (triarylsulfonium hexafluoroantimonate salts).

Side chain cleavage (deprotection) mechanism of MAdMA-*co*-GBLMA in presence of acid and heat treatment

Scheme 1. Side-chain cleavage scheme of model resist system poly(MAdMA-*co*-GBLMA). Side-chain cleavage occurs through acidolysis as MAdMA is converted to methylene adamantane.
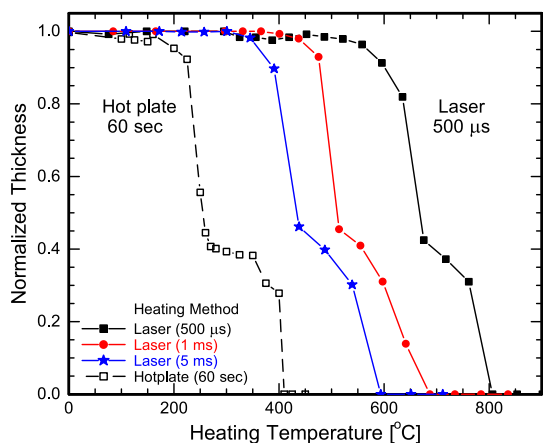

Figure 3. Film thickness remaining as a function of temperature showing the thermal stability limits under hot-plate (60 s) and laser (0.5, 1, and 5 ms) heating. Reducing the heating duration by 5 orders of magnitude increases the temperature stability of the polymer by 400 °C.

peak temperature for a 60 s hot-plate bake and for laser bake thermal cycles of 0.5, 1, and 5 ms. For all heating times, the thickness of the film decreases by 60% at intermediate temperatures due to decomposition of thermally sensitive side groups.[12] As the heating temperature increases, C—C bonds in the backbone are broken and the film completely decomposes. The shape of the curves are similar, but the ultimate thermal stability of the polymer is increased by ~400 °C at 500 μs, showing that even sensitive organic molecules can be characterized at temperatures far above conventional use limits.

To take advantage of the extended temperature regime, reaction kinetics and acid diffusion, both critical properties of a resist, were investigated. These chemical kinetic rates have been extensively investigated on time frames of seconds to minutes using conventional heat sources (hot-plates), but at shorter time frames and higher temperatures the behavior is essentially unknown.[2,13] Polymer side-chain cleavage kinetics were measured using dissolution curves, plotting the thickness of resist remaining after development as a function of UV dose (mJ/cm^2). The dose to clear (E_0) is a function of both heating time and temperature[13] with representative data shown in

Figure 4a for a 60 s hot-plate and a 500 μs laser at various temperatures. Owing to the large difference in heating time (500 μs versus 60 s), laser bake requires much higher temperatures to achieve a response similar to the hot-plate (e.g., compare laser curve at ~420 °C with the 150 °C hot-plate curve).

To summarize data over a range of temperatures and times, isotherms on a log−log E_0 *versus* heating time are plotted in Figure 4b. For laser bake, the temperature varies continuously during heating, and an effective time at temperature must be used. This is defined as the duration of an equivalent isothermal process at the peak temperature and is dependent on the activation enthalpy of the underlying process and the actual temperature−time profile (see Supporting Information for detailed calculation). For side chain cleavage rates with an activation enthalpy of 21 kJ/mol, the effective time is $4.0\tau_{dwell}$.

At a given temperature, E_0 increases as heating time decreases consistent with a kinetic limit for side-chain cleavage. While both laser and hot-plate data exhibit substantial temperature dependence, they exhibit remarkably different behavior with respect to the heating duration. The data suggest a power law dependence $E_0 \propto t^n$, as shown by the solid line fits. For hot-plate heating, the slope is -0.25 ± 0.05 at 115 °C (just above $T_g \approx 110$ °C) and decreases slightly with temperature until the resist begins to decompose above ~190 °C where the slope becomes ill-defined. In contrast, the slope for laser data is independent of temperature and time at -1.0 ± 0.2.

It is difficult to reconcile these data with simple Arrhenius activated kinetics. For modeling it is more appropriate to consider the time required, at fixed temperature, to achieve the necessary side-chain cleavage as a function of the exposure dose (initial concentration of acids). The data suggest a form $E_0^n \times t = C(T)$ where n is the power law exponent (=slope^{-1}) and $C(T)$ is a constant dependent on the peak temperature and heating conditions. The exponent is ~4 for hot-plate and ~1.0 for laser. This unity exponent for laser bake is consistent with a simple first-order kinetically limited process for side-chain cleavage − halving the number of acids (catalysts) present in the system
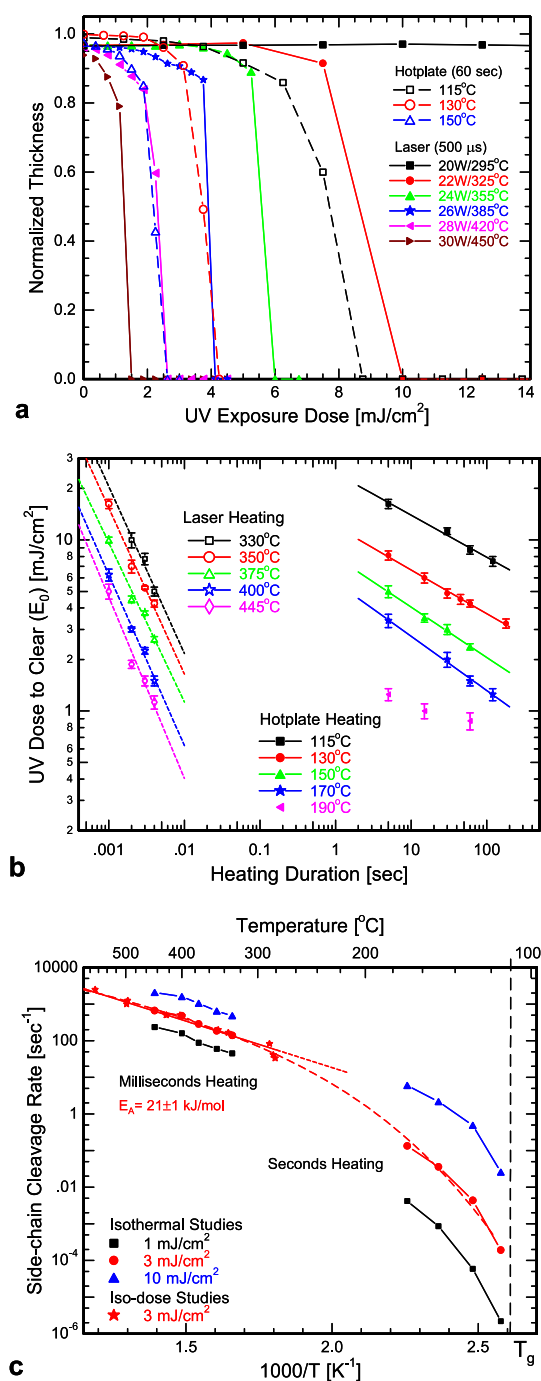
Figure 4. Comparison of dose to clear (E_0) between hot-plate and LB heating. (a) Normalized thickness *versus* UV dose for HP and 500 μs LB. (b) Isotherms of E_0 *versus* time. Data exhibit different slopes for HP and LB heating. (c) Arrhenius plot of reaction rate (panel b) for E_0 = 1, 3, and 10 mJ/cm^2.

requires twice the time to achieve the same number of cleaved segments. In contrast, halving the exposure dose with hot-plate heating increases the time required by 16 times — suggesting a fourth-order reaction mechanism or more complex kinetic pathways. FTIR measurements of the ester and carbonyl peaks (from the side-chain) after laser bake exhibit the same decay observed in hot-plate experiments[7] indicating a

similar fundamental underlying chemical reaction (see Supporting Information).

The behavior observed for this resist system is not unique. Similar behavior was observed with another resist system consisting of a copolymer of 4-hydroxy-styrene (HOST) and *tert*-butyl acrylate (TBA),[14] whose chemical reactions involve a different mechanism with conversion of an ester to carboxylic acid. Slopes (corresponding to Figure 4b), are *ca.* −0.5 for hot-plate and *ca.* −1.1 for laser heating. The simple first-order behavior of the laser regime appears universal while the complex hot-plate kinetic regime may vary with polymer systems and the relative temperature deviation $T - T_g$.

As underlying reactions are expected to be thermally activated, Figure 4c shows the log of the side-chain cleavage rate (over 10 orders of magnitude) as a function of inverse temperature for constant acid catalyst concentrations (corresponding to UV exposures of 1, 3, and 10 mJ/cm^2). At high temperatures (300−600 °C), the rates exhibit Arrhenius behavior with an activation enthalpy E_A = 21 ± 1 kJ/mol, consistent with side-chain protonation, acidolysis, and/or acid regeneration[15] steps in the cleavage. However, as the system approaches T_g (~110 °C), the cleavage rates decrease rapidly with a fingerprint typical of dynamics associated with segmental polymer motion near T_g. Between these limiting regimes, a crossover range exhibiting a power law dependence is expected.[16] At even lower temperatures below T_g, the behavior is expected to return again to Arrhenius behavior but with an activation enthalpy in the range of 100 kJ/mol.[17,18] Direct observation of the transitional behavior between segmental dynamics above T_g and the newly observed Arrhenius behavior with low activation enthalpy at high temperature is possible only because of the ability to extend the temperature using this laser heating technique.

The limiting high and low temperature behavior may be associated with a common kinetic process coupled to the polymer segmental dynamics, but it is more likely that two distinct kinetic processes, acting sequentially in the cleavage, are rate-limiting. At low temperatures the limiting step is likely acidolysis to cleave the side-chain, which would exhibit both a high activation enthalpy (observed below T_g[17,18]) and coupling to segmental-like dynamics associated with conformational changes in the polymer backbone during this step (Scheme 1). At high temperatures well-above the glass transition, we believe the backbone dynamics are no longer rate-limiting, but the formation of the double-bond and acid regeneration associated with the final formation of the methylene adamantane limits the rates. This structural stabilization is expected to be relatively athermal consistent with the observed low activation enthalpy at high temperatures.

A shift in the underlying rate-limiting reaction step would also potentially explain the observed power-law exponent difference. With different steps in the reaction chain critical in the two time/temperature regimes, it is reasonable to expect a shift from simple first-order kinetics at high temperature to a more complex kinetic process involving coupling to segmental dynamics of the polymer chain and reaction byproducts at low temperature.

While a shift in rate-limiting steps is most likely, other mechanism shifts could produce similar changes in the apparent activation enthalpy at low and high temperatures. Intermediate steps in the stabilization of the final byproduct methylene adamantane may act as acid traps at low temperatures, increasing the apparent activation enthalpy. Such a trap would act with the rate-limit shift to give rise to both the activation enthalpy change and the lack of first order kinetics at low temperature.

Given the complexity of the low and high temperature regimes, diffusion of the photoacids (another step in the reaction chain) must also be considered. Substantial changes in the acid mobility would directly impact polymer side-chain cleavage kinetics. In addition, in contrast to complex side-chain cleavage kinetics, diffusion is a much simpler random walk problem, albeit potentially impacted by structural changes arising from the cleavage kinetics. Bilayer structures, consisting of an acid-containing top layer and acid-free bottom layer, were treated by hot-plate or laser after UV exposure.[14] Acids initially only present in the top layer diffuse and subsequently cleave side-chains in the lower film as well. Thickness loss of the bottom layer after development thus measures the proton diffusion as shown in Figure 5a. T_g differences in the bilayers impacts the localized acid motion, but not the limiting diffusion distance in these films (see Supporting Information). Diffusion becomes significant on these length scales for hot-plate temperatures above 130 °C and for laser temperatures above ~385 °C (26 W).

The acid diffusivity $D = (\Delta x^2/4t)$, based on diffusion from an initial concentration step,[19] is shown in Figure 5b as a function of inverse temperature. For a laser bake, the effective time at temperature is ~$1.2\tau_{dwell}$ based on an activation enthalpy of ~175 kJ/mol (see Supporting Information for detailed calculation). At low temperatures (but still above $T_g \approx$ 110 °C), acid diffusion in similar polymer systems has been shown to follow the Williams−Landel−Ferry (WLF) model, which links diffusion to free volume near the glass transition temperature.[20,21] As with the side-chain cleavage dynamics, while the low temperature regime (<280 °C) appears linked to free volume near the glass transition, the high temperature regime (>300 °C) exhibits Arrhenius behavior. Surprisingly however, in contrast to the chain cleavage dynamics, at high temperatures the diffusivity is accelerated
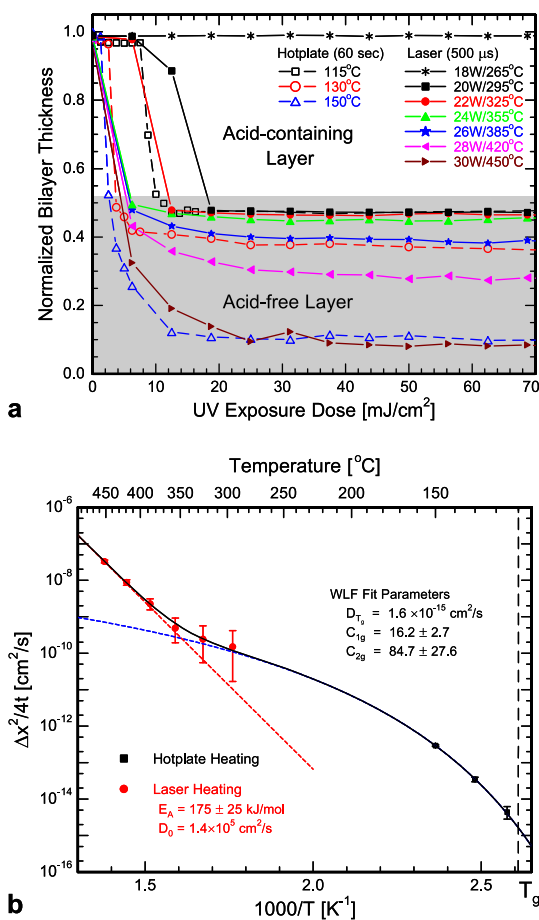

Figure 5. Photoacid diffusivity measurements. (a) Bilayer structure consisting of a top layer containing a photoacid generator and a resist-only bottom layer. Heating was for 60 s (HP) or 500 μs (LB). (b) Plot of measured acid diffusivity. Arrhenius behavior (red dotted line) is observed at high temperatures while WLF model (blue dotted line) is obeyed at low temperatures. The fit provided by a combined WLF and Arrhenius model is represented by the solid black line.

and exhibits an activation energy significantly higher than expected from extrapolation of the WLF behavior (compare with Figure 4c). As these mechanisms act in parallel, we model the overall diffusivity as a sum of an Arrhenius term and the WLF model:

$$D = D_{Arrhenius} + D_{WLF}$$

$$= D_0 \exp\left(-\frac{E_A}{kT}\right) + D_{T_g}\exp\left(\frac{C_{1g}\cdot(T - T_g)}{C_{2g} + (T - T_g)}\right) \quad (1)$$

where D_{T_g} is the diffusivity at T_g. With T_g fixed at 110 °C, fits to the data yield $D_0 = 1.4 \times 10^5$ cm^2/s, $E_A = 175 \pm$ 25 kJ/mol, $D_{T_g} = 1.6 \times 10^{-15}$ cm^2/s, $C_{1g} = 16.2 \pm 2.7$ and $C_{2g} = 84.7 \pm 27.6$. These WLF fit parameters are well within the range expected for similar polymer systems,[22,23] and the crossover from WLF to Arrhenius behavior at 350 °C occurs more than 200 °C below the thermal decomposition limit (Figure 3). However, the Arrhenius activation energy of 175 kJ/mol is significantly higher than expected for typical diffusive

processes in polymer liquids far above T_g (~60 kJ/mol).[24] Ultimately, the remarkable agreement of this simple model with the experimental data over eight orders of magnitude is compelling evidence for the validity of this linked WLF and Arrhenius model. Indeed, observation of this unexpected crossover is possible only because of the extremely large temperature span enabled by this submillisecond heating technique.

While a transition from segmental dynamics near T_g to Arrhenius behavior at high temperature has been used to explain these data, several alternatives associated with the substantial differences between hot-plate and laser heating were also considered. Photoinduced chemical processes, unlikely given the 0.12 eV CO_2 photons, were shown to be negligible for power levels up to 20 W/cm^2. Similarly, while there is potential for relaxation of UV induced defects during the 100 K/s ramp rate of a hot-plate that might be bypassed with the 10^5 K/s ramp rate of laser heating, the laser bake behavior was unmodified after a short (15 s) hot-plate bake indicating negligible film changes during slow temperature ramping. Ramp rate may still be a critical factor as it may influence mechanical relaxation mechanisms above T_g, or induce kinetic changes from reaction byproducts that have insufficient time to escape during laser heating.

CONCLUSIONS

We have demonstrated the ability to extend the temperature range for characterization and processing of polymers and small molecule systems by at least 400 °C using transient laser heating on submillisecond to millisecond time frames. Using a model system based on a chemically amplified photoresist, chemical reaction kinetics were characterized over nearly 10 orders of magnitude covering temperatures from 115 to 560 °C. The transition from kinetics defined by local polymer segmental dynamics at low temperature to kinetics associated with the equilibrium liquid at high temperature were quantified. In the low temperature regime, side-chain cleavage kinetics exhibited a power law scaling suggesting a fourth-order reaction while the high temperature regime was first order. In the high temperature regime, the activation enthalpy was 21 ± 1 kJ/mol for side-chain cleavage and 175 ± 25 kJ/mol for acid diffusion. Across nearly 8 orders of magnitude, the diffusion was accurately modeled using combined WLF and Arrhenius behaviors. These observed behaviors have potentially critical implications for the processing and characterization of a broad range of complex polymers. More generally, the use of laser induced heating opens up an entirely new area for investigation of polymer and small molecule reaction kinetics in the near-solid state at extended temperatures.

MATERIALS AND METHODS

Temperature Calibration. Accurate peak temperature measurements during millisecond heating are critical for this work. Time-resolved temperatures were inferred from the resistance change of thin-film (50 nm) platinum resistors (thermistors fabricated on equivalent Si wafers) with an area (<10^{-5} cm^2) that minimally perturbed the incident CO_2 laser.[25] The resistance of Pt is linearly proportional to temperature and was measured with >10 kHz bandwidth. Absolute resistances were calibrated at powers corresponding to experimentally observed melting of silicon (1414 °C) and of micrometer size gold dots (1064 °C) (see Supporting Information).

Sample Preparation and Acid Generation Using UV Exposures. 2-Methyl-2-adamantyl methacrylate-co-γ-butyrolactone-2-yl methacrylate (MAdMA-co-GBLMA), and triarylsulfonium hexafluoroantimonate salt (THS) were commercially obtained from Mitsubishi Rayon Co., Ltd. and Sigma Aldrich. Poly(MAdMA-co-GBLMA) containing 5 wt % THS were vigorously stirred overnight in propylene glycol monomethyl ether acetate (PGMEA). Target thickness for all films was 100 nm. All samples were soft baked on a vacuum hot-plate at 130 °C for 90 s to remove the PGMEA solvent. Resist layers and bilayers were exposed to deep UV ($\lambda = 235-260$ nm) irradiation. Following either hot-plate or laser heating, samples were developed in 0.26 N TMAH for 60 s at room temperature.

For diffusion studies, bilayer resist samples with a THS-containing top layer (acid generating layer) and a THS-free bottom layer were fabricated using a polydimethylsiloxane (PDMS) stamping technique. First, a PDMS stamp (~5 mm thickness and ~90 mm diameter) was prepared and spun with a 100 nm of THS-containing resist solution. Second, a silicon wafer substrate was spun with THS-free resist solution to achieve ~100 nm thick film. Both substrates were soft baked on a vacuum hot plate at 130 °C for 90 s. The PDMS with the THS-containing layer was then stamped onto the wafer and soft baked for an additional 20 s at 90 °C for adhesion between the two polymer films prior to the removal of the PDMS stamp. Under UV exposure, the THS in the top layer generated free acids that potentially can diffuse into the bottom layer upon subsequent heat treatment.

Because of the potential for changes in the diffusion behavior from differing glass transition temperatures in the top and bottom layers, diffusion measurements were also performed on bilayers where both layers contained the THS photoacid generators. In these experiments, the top layer was exposed under UV to generate free acids for diffusion prior to lamination with the bottom layer. At high UV doses, the diffusion distance observed in these bilayers was essentially the same as that measured in films without THS. However, this saturation was observed at lower UV doses for these bilayers.

Heat Treatment. Photogenerated acids were introduced by exposing resist-coated wafers to UV irradiation (235–260 nm) at doses of 0.1–12 mJ/cm^2. Samples were subsequently heated under either isothermal conditions on a vacuum hot-plate or using the submillisecond laser heating system. In the presence of a free acid and sufficient temperature/time, a side-group of MAdMA is cleaved and converted to methacrylic acid, which subsequently regenerates the acid as it stabilizes to methylene adamantane. Following either hot-plate or laser heating, samples were developed in 0.26 N tetramethylammonium hydroxide (TMAH) for 60 s at room temperature.

Conflict of Interest: Thompson is a consultant for Ultratech, a company involved in manufacturing equipment for millisecond

annealing. The outcome of this research may be of interest to, or may be beneficial to, Ultratech. The authors declare no other competing financial interest.

Supporting Information Available: Temperature measurement of laser heating, effective time calculation, characterization (FTIR, DSC), fabrication techniques, and data processing included. This material is available free of charge *via* the Internet at http://pubs.acs.org.

REFERENCES AND NOTES

1. Kodambaka, S.; Tersoff, J.; Teuter, M. C.; Ross, F. M. Germanium Nanowire Growth below the Eutectic Temperature. *Science* **2007**, *316*, 729–732.
2. Ito, H. Chemical Amplification for Microlithography. *Adv. Polym. Sci.* **2005**, *172*, 27–245.
3. Lee, B. S.; Burr, G. W.; Shelby, R. M.; Raoux, S.; Rettner, C. T.; Bogle, S. N.; Darmawikarta, K.; Bishop, S. G.; Abelson, J. R. Observation of the Role of Subcritical Nuclei in Crystallization of a Glassy Solid. *Science* **2009**, *326*, 980–984.
4. Yamamoto, T.; Kubo, T.; Sukegawa, T.; Takii, E.; Shimamune, Y.; Tamura, N.; Sakoda, T.; Nakamura, M.; Ohta, H.; Miyashita, T.; *et al.* Junction Profile Engineering with a Novel Multiple Laser Spike Annealing Scheme for 45-nm Node High Performance and Low Leakage CMOS Technology. *Int. Elec. Devices Meet.* **2007**, *1*, 143–146.
5. Fakhraai, Z.; Forrest, J. A. Measuring the Surface Dynamics of Glassy Polymers. *Science* **2008**, *319*, 600–604.
6. Cameron, J. F.; Willson, C. G.; Fréchet, J. M. J. Photogeneration of Amines from α-Keto Carbamates: Photochemical Studies. *J. Am. Chem. Soc.* **1996**, *118*, 12925–12937.
7. Kang, S.; Vogt, B. D.; Wu, W. L.; Prabhu, V. M.; VanderHart, D. L.; Rao, A.; Lin, E. K. Characterization of Compositional Heterogeneity in Chemically Amplified Photoresist Polymer Thin Films with Infrared Spectroscopy. *Macromolecules* **2007**, *40*, 1497–1503.
8. Dektar, J. L.; Hacker, N. P. Photochemistry of Triarylsulfonium Salts. *J. Am. Chem. Soc.* **1990**, *112*, 6004–6015.
9. Vogt, B. D.; Kang, S.; Prabhu, V. M.; Lin, E. K.; Satija, S. K.; Turnquest, K.; Wu, W. L. Measurements of Reaction-Diffusion Front of Model Chemically Amplified Photoresists with Varying Photoacid Size. *Macromolecules* **2006**, *39*, 8311–8317.
10. Lin, E. K.; Soles, C. L.; Goldfarb, D. L.; Trinque, B. C.; Burns, S. D.; Jones, R. L.; Lenhart, J. L.; Angelopoulos, M.; Willson, C. G.; Satija, S. K.; *et al.* Direct Measurement of the Reaction Front in Chemically Amplified Photoresist. *Science* **2002**, *297*, 372–375.
11. Kang, S.; Wu, W. L.; Choi, K. W.; Silva, A. D.; Ober, C. K.; Prabhu, V. M. Characterization of the Photoacid Diffusion Length and Reaction Kinetics in EUV Photoresists with IR Spectroscopy. *Macromolecules* **2010**, *43*, 4275–4286.
12. Thompson, L. F.; Willson, C. G.; Bowden, M. J. Introduction to Microlithography. *ACS Professional Reference Book*; American Chemical Society: Washington DC, 1994; pp 212–232.
13. Malik, S.; Eisele, J.; Whewell, A.; Ferreira, L.; Holt, T.; Bowden, M. Post-exposure Bake Temperature Considerations for High Activation Energy Resist Systems. *J. Photopolym. Sci. Technol.* **2000**, *13*, 513–518.
14. Ito, H.; Breyta, G.; Hofer, D.; Sooriyakumaran, R. Environmentally Stable Chemical Amplification Positive Resist: Principle, Chemistry, Contamination Resistance, and Lithographic Feasibility. *J. Photopolym. Sci. Technol.* **1994**, *7*, 433–488.
15. Benson, S. W. *Thermochemical Kinetics: Methods for the Estimation of Thermochemical Data and Rate Parameters*; John Wiley & Sons: New York, 1976; pp 17–320.
16. Chen, K.; Saltzman, E. J.; Schweizer, K. S. Molecular Theories of Segmental Dynamics and Mechanical Response in Deeply Supercooled Polymer Melts and Glasses. *Annu. Rev. Condens. Matter Phys.* **1994**, *1*, 277–300.
17. Wallraff, G; Hutchinson, J.; Hinsberg, W.; Houle, F.; Seidel, P.; Johnson, R. Oldham, W. Thermal and Acid-Catalyzed Deprotection Kinetics in Candidate Deep Ultraviolet Resist Materials. *J. Vac. Sci., Technol. B* **1994**, *12*, 3857–3862.
18. Hinsberg, W. D.; Houle, F. A.; Sanchez, M. I.; Wallraff, G. M. Chemical and Physical Aspects of the Post-exposure Baking Process used for Positive-Tone Chemically Amplified Resists. *IBM J. Res. Dev.* **2001**, *45*, 667–682.
19. Gusev, A. A.; Müller-Plathe, F.; van Gunsteren, M. F.; Suter, U. W. Dynamics of Small Molecules in Bulk Polymers. *Adv. Polym. Sci.* **1994**, *116*, 207–247.
20. Williams, M. L.; Landel, R. F.; Ferry, J. D. The Temperature Dependence of Relaxation Mechanisms in Amorphous Polymers and Other Glass-Forming Liquids. *J. Am. Chem. Soc.* **1955**, *77*, 3701–3707.
21. Stewart, M. D.; Somervell, M. H.; Tran, H. V.; Postnikov, S. V.; Willson, C. G. Study of Acid Transport using IR Spectroscopy and SEM. *Proc. SPIE* **2000**, *3999*, 665–679.
22. Ferry, J. D. *Viscoelastic Properties of Polymers*; John Wiley & Sons: New York, 1980; pp 264–315.
23. Priestley, R. D.; Vroadbelt, L. J.; Torkelson, J. M.; Fukao, K. Glass Transition and α-Relaxation Dynamics of Thin Films of Labeled Polystyrene. *Phys. Rev. E* **2007**, *75*, 061806.
24. Bueche, F. *Physical Properties of High Polymers*; Interscience: New York, 1962; pp 90–93.
25. Iyengar, K.; Jung, B.; Willemann, M.; Clancy, P.; Thompson, M. O. Experimental Determination of Thermal Profiles during Laser Spike Annealing with Quantitative Comparison to 3-Dimensional Simulations. *Appl. Phys. Lett.* **2012**, *100*, 211915–1–3.